applied sciences

MDPI

Article

Experimental Study on a Reinforced Concrete Element to Extract the Durability Index with the Automated Visualization

Seyed Mohammad Sadegh Lajevardi [1], Fereidoon Moghadas Nejad [2,*] and Mehdi Ravanshadnia [1]

[1] Department of Civil Engineering, Science and Research Branch, Islamic Azad University, Tehran 1477893855, Iran
[2] Department of Civil and Environmental Engineering, Amirkabir University of Technology, Tehran 1591634311, Iran
* Correspondence: moghadas@aut.ac.ir

Abstract: Reinforced concrete (RC) durability is a crucial feature to estimate long-term quality and structural performance. The degradation model is vital for the resource planning of maintenance projects. This model will extract data by updating the status of structures and trending the components' state over time in terms of durability. Surface erosion, spalling, cracks, and other defects exposed on RC components lead to increase factors adversely affecting concrete durability in structures. This research presents an approach based on automated visualization for extracting quantitative indexes as well as visual inspection without the subjective interspersion of humans or probable human errors during the inspection. The durability index (D_i) will extract according to damage probability and defects growth in order to extract the severity of failure and risk. Measurement operation by automated software has been double-checked by manual measurement tools, and data will verify randomly in this method. The results show that, in this component, the damaged area increases by 24% after a definite time. According to degradation models, this component may pass the relative thresholds for the limit for the state of operations to fail. This significant difference between expected time and designing time determines the D_i, equal to 5 out of 10.

Keywords: durability; reinforced concrete; automated visualization; risk

Citation: Lajevardi, S.M.S.; Moghadas Nejad, F.; Ravanshadnia, M. Experimental Study on a Reinforced Concrete Element to Extract the Durability Index with the Automated Visualization. *Appl. Sci.* **2022**, *12*, 9609. https://doi.org/10.3390/app12199609

Academic Editors: Valerio De Martinis and Raimond Matthias Wüst

Received: 24 June 2022
Accepted: 9 August 2022
Published: 24 September 2022

1. Introduction

Since time immemorial railway infrastructure networks were developed in industrial countries, they have been based the demands of transferring loads and passengers. As such, passengers and infrastructure owners are the most substantial stakeholders and it is necessary to undertake corrective actions in line with stakeholders' demands. For instance, based on operators' mandates and passengers' expectations, enhancing the convenience of travel and reducing time travel duration is essential. Therefore, automation in railway infrastructure quality control is an important factor in reaching the mentioned goals with a minimum risk for inspectors. Additionally, reducing the number of unexpected failures during operations leads to reducing the train emergency stops and increasing the number of successful journeys. On the other hand, the ageing process over time leads to quality loss because of environmental aspects and chemical reactions inside the materials. Thus, the conditions of structures have to be updated in terms of quality. Meanwhile, routine inspections play a crucial role in maintenance activities [1].

As a first step, gathering data is necessary for a researcher in the field of quality control. Based on intermittent train movements with short intervals, inspections between operations are necessary for safety. However, many crises threaten inspectors during the operation if they follow traditional inspection methods. Defect growth estimation denoted by automatic monitoring methods through various sorts of sensors prepares a database for finding the durability index. In this manner, structural health monitoring (SHM) methods update a structural component's state based on the prepared database [2]. The SHM utilizes various

methods, such as damages and cracks detection using images, vibration indications, and abnormal measurement diagnosis [3]. In this manner, several sensors (for factors such as humidity, temperature, pressure, load, potential hydrogen (PH), hardness, chemical composition, acoustic emission (AE), and others) have been employed for data gathering and damage detection [4,5]. AE was used for damage monitoring in reinforced concrete structures [6,7]. In this way, AE is applied to highlight internal damage progress [8]. However, the complex fracture and defects cannot be efficiently categorized and rated by measuring deterioration with certain monitoring methods, such as visual sensors, but these sensors can detect surface defects and mechanical features [8]. One of the famous tests for examining concrete elements is a visual inspection which uncovers damages, and automated visual inspections measure the defect growth. Since real-time monitoring is necessary for reliability assessment, automated visualization is an essential tool for inspectors to evaluate objects without human error, combined with regular inspections.

Analyzing data in automation systems has been carried out by researchers using intelligent approaches [9]. There are three levels desirable for SHM during operations. The first level focuses on defect detection and alarms for the operator. The second level prepares a baseline for comparing elements and their priority. The third level guides decision makers to estimate and forecast future demands through trends. In this manner, the semantic web layer acts as the "brain" to provide the basis for determining defects [10]. However, this research presents risk as a basic factor for automation in decision-making after image processing and data gathering.

Electrical conductivity is an aspect in terms of structural health monitoring methods which can estimate the durability of reinforced concrete [11]. However, the durability of reinforced concrete after risk analysis is not connected with image processing based on the surface degradation status within a specific time window. This research will focus on this gap to improve condition-based maintenance.

1.1. Structural Health Monitoring

Several tools, such as ground penetrating radar (GPR), ultrasonic (UT) tools, X-ray tubes, accelerometers, moisture meters, linear variable differential transformers (LVDT), flat jacks, and other measuring tools, are appropriate for finding the features and behavior of a structure. According to recent research, some of these are suitable for uncovering internal damage and some can be utilized for external damages based on feature comparison before and after degradation. To find the overall quality state of the structure, visual inspection was selected to compare to other non-destructive tests (NDT). Visual inspection is not expensive, and it is appropriate for finding critical zones in the structure. This paper is not focused on expensive tools for monitoring structures. Therefore, an automated visual test was selected to develop the decision-making system at a lower cost in the software field [12]. Meanwhile, the recent research in the literature review refarding to this subject shows software for data processing supports not only data extracted from a charge-coupled device (CCD) or a supplementary metal–oxide semiconductor (CMOS) sensors but also supports many other sensors, such as ground penetrating radar (GPR) [13,14]. In fact, signal processing after receiving data from hardware is essential for software analysis and decision-making based on data. Therefore, the visual sensor output is a type of signal for operators, such as other structural health monitoring tools output.

Therefore, due to the development of the railroad network, automation in monitoring is avoidable for inspectors through the precise planning and codification of defect types and their locations, regarding corrective action [15,16]. Also, several studies try to develop decision support systems by processing data after the act of collecting [17–22].

1.2. Durability

The durability of concrete may be defined as the ability of the concrete to bear potential chemical attacks, crushing, weathering, and abrasion based on the structure permeability for gas and water, absorptivity, initial absorption capacity, water tightness, diffusion, and

others [23]. Meanwhile, durable concrete maintains its desired engineering properties during operation. For instance, the durability index for aggregate is a value which represents the relative resistance of the material to produce detrimental clay when subjected to the suggested mechanical degradation techniques [24]. The design service life of a structure should be prepared based on the requirements of the owners and operators. The service life of an important and large bridge may be 50 years to 100 years [25]. Cutting-edge design for durability deals with the inherent uncertainties in material and environmental features [26,27]. Non-destructive tests (NDT) assess the quality of concrete in terms of durability. Several common defects, such as the corrosion of steel in concrete, are related to durability. Additionally, recent research shows some non-destructive electrochemical tools are useful and commonly used for monitoring these types of defects, especially in corrosion investigations. Electrical resistivity is an NDT tool used to measure the durability of concrete along with its quality. The electrical resistance of an object is a measure of its opposition to the flow of electric current. This feature of concrete shows its durability based on void connectivity [28,29]. Currently, this research aims at uncovering the D_i estimation and the possibilities of condition monitoring, along with subsequent data-gathering based on image processing tools. Therefore, this research has prepared a maintenance plan for a case study based on SHM results and the extracted D_i according to the semantic approach. Finding critical elements in the structure and estimating their lifetime is the outcome of this maintenance plan. Finding critical elements in the structure will mostly involve the filtering of the enormous dataset in terms of quality. The rate of growth for progressive defects and cracks is a piece of evidence to assist in finding critical concrete elements in terms of their quality comparison. Numerous superfluous and costly data will be eliminated from the input dataset with this approach. This means that durable elements will not need to be checked by frequent inspections within short timeframes. Meanwhile, critical elements with expanding damage are important for inspectors and maintenance managers. Finally, the main contribution of this research work is presenting a relative index based on damage detection by monitoring changes and representing optimized maintenance plans by considering the durability of concrete elements as well as other aspects of quality and critical zones.

2. Methodology

Although the reliability index is a parameter that is known to designers, this quantitative index has been neglected by maintenance managers. Risk assessment and its related reliability index are parameters that allow the supporting of infrastructure owners to prepare a decision support system for corrective activities. To measure damage propagation, it is inevitable that automation tools will be used, leading to quantitative results. This research focuses on extracting the risk index to estimate part of a degradation model of concrete elements in terms of their durability. Since this research aims to combine the automated damage detection of RC components with risk severity and durability content, it is necessary to consider several image processing methods and the technical limit states of concrete elements. Therefore, this research applies several tools to the aim of finding D_i as follows.

2.1. Software and Hardware Details for SHM

According to Eurocode 2 and ACI 224R-0, the limit state of crack width is considered 0.3 mm [30,31]. Moreover, RC components with spalling defects, as well as exposed rebar, are a risk for RC structure durability. Therefore, based on an initial visual test, the selected object for this research has a potential risk in terms of the probability of defects in this RC structure [32]. The monitoring set-up for the RC component is illustrated in Figure 1.

Figure 1. Data gathering process.

The case study location was established at the end of the bridge's abutment. This is a non-level intersection of the road and railway bridge placed in the west urban area of the Tehran subway. The drainage barbican is not adequately isolated from the concrete surface, and the wastewater in the urban area leads to carbonation and damage propagation during operation.

While gathering data, the camera had to be fixed under natural lighting on a sunny day. Data gathering was performed using a camera with a CMOS sensor and 22.3 × 14.9 mm dimension. The specification of computer processors and language programing during the data analysis are as follows:

- ✓ Core i7 Processor;
- ✓ 16 GB of random access memory (RAM);
- ✓ C# Programming language.

This research desired to find the damage propagation based on automated visual inspection. Therefore, edge detection was applied to detect and measure the damaged area to estimate the durability index. Edge detection steps are as follows [33]:

- ✓ Filtering and Enhancement—Filter image to improve the performance of the edge detector;
- ✓ Detection—Finding edges by defining the threshold with the minimum thickness (1 pixel);
- ✓ Localization—locate the edge accurately in the photo.

2.2. Image Processing Method

In the computer vision, different methodologies were exploited to solve practical problems, such as object recognition. An object to detect the displacement of an element or damaged area in a structural component [34]. Surface cracks and surface foreign objects can simply make a large number of incorrect edge detections when the fringe phenomenon is generated by the uneven distribution through exploiting a typical differential edge detector. Therefore, it was necessary to design a detection operator that is capable of reducing noise [35,36]. Kayyali, Harris and Stephens/Plessey/Shi–Tomasi, SUSAN, Shi and Tomasi, level curve curvature, FAST, laplacian of Gaussian, difference of Gaussians, determinant of Hessian, MSER, PCBR, grey-level blobs, automated, independent component analysis,

isomap, latent semantic analysis, partial least squares, semidefinite embedding, auto-encoder, nonlinear dimensionality reduction, and principal component analysis (kernel PCA and multilinear PCA) are the methods which were applied for image processing. Some of the most important methods for data analysis are as follows:

2.2.1. Canny

Canny's edge recognition algorithm is a conventional technique for edge detection in grey-scale images [37]. After noise reduction, it is necessary to enhance the quality of the extracted image from the previous step with a smooth mathematical tool called Gaussian. Additionally, detection and localization criteria were found based on the formula that follows. First, every signal is transferred to the noise ratio and then localizes the criteria. Let the impulse response of the filter be $f_{(x)}$ and denote the edge itself through $G_{(x)}$. Then the response of the filter to this edge at its center, H_G, is given by a convolution integral [33], assuming the filter has a finite impulse response bounded by [−W, W].

$$H_G = \int_{-W}^{+W} G_{(x)} f_{(x)} dx \tag{1}$$

This method detects by extracting useful structural information from various visual objects and dramatically reduces the amount of data to be processed. The two significant features of this technique are the development using the double thresholding of the gradient image and non-maximum suppression [10].

2.2.2. Fuzzy Operator

Edge pixels are recognized by evaluating a local change in intensity followed by thresholding. The change in intensity may be measured by defining the first derivative of the image function. The rate of change of a 2D image intensity function, *f(x, y)*, is given by the gradient vector as follows [38]:

$$\nabla f = \begin{bmatrix} \frac{\partial f}{\partial x} \\ \frac{\partial f}{\partial y} \end{bmatrix} = \begin{bmatrix} G_x \\ G_y \end{bmatrix} \tag{2}$$

where G_x and G_y indicate the rate of intensity change along the horizontal (x-axis) and vertical (y-axis) directions. The rate of the gradient vector ∇f refers to the rate of change in intensity at the pixel location (x, y) as follows:

$$G(x,y) = \sqrt{G_x^2 + G_y^2} = \sqrt{\left(\frac{\partial f}{\partial x}\right)^2 + \left(\frac{\partial f}{\partial y}\right)^2} \tag{3}$$

This method has been used for detecting defects after imaging in the industry [39]. Additionally, this attitude is a developed intelligence-supportive system for decision-making and classification [40].

In this research, damage detection and data processing were carried out using this logical tool to obtain the D_i for the RC component. This technique presents the best results with the highest resolution to compare to the other remaining techniques previously mentioned when checking the damage propagation rate.

2.2.3. Sobel Operator

This operator is a tool for image processing and crack recognition. It has been applied to the elimination of isolated noise spots, the extraction of crack edge evidence, and the improvement of the positioning accuracy of crack boundaries. Furthermore, according to the image feature of the bridge crack edge, the target crack is identified and classified by this method [41].

This method has been utilized for estimating the edge strength of every pixel point in the input image. Therefore, the intensity gradients G_x and G_y in the horizontal and vertical directions are determined at every pixel (x, y) in the image. The kernels can be exploited discretely in the input image to produce the separate measurements of the gradient component in each orientation (call these G_x and G_y).

$$|G| = \sqrt{G_x^2 + G_y^2} \tag{4}$$

$$\theta = arctan\left(\frac{G_y}{G_x}\right) \tag{5}$$

Orientation 0 is taken to mean that the direction of maximum contrast from black to white runs from left to right on the image, and other angles are measured anti-clockwise from this [42].

2.2.4. Prewitt Operator

The Prewitt kernels are simpler to implement than the Sobel kernels, but the slight computational difference between them typically is not an issue [42]. The Prewitt technique is a suitable tool for data processing based on the results of intensity functions. The outcomes of this technique were applied for edge detection where the gradient of the intensity function had an extreme value [43].

2.2.5. Research Operators

In this research, after the preparation of the grey scale from a pure image, the fuzzy, the Sobel, and then the Prewitt operators were employed for damage detection extraction. Since these methods and operators have been applied in recent research, they were utilized to find the dimension of the damage in the present research. Based on this step, output damage propagation can estimate the severity of failure and D_i in the bridge.

2.3. Probabilistic-Based Structural Assessment

Based on the RC elements limitation, it is possible to assess the durability of RC. For this reason, the probability of failure for the component is calculated in this segment.

2.3.1. Probability of Failure

In this research, the probability of failure illustrates a defect in the overall view of the bridge and is a failure of the component. This means that the failure of structural elements does not necessarily lead to overall structure failure because it might be possible to transfer load-bearing onto other parallel structural elements.

2.3.2. Severity of Failure

Defect propagation is a sign of the severity of failure (S_f) during operations for risk assessment. In this research, it is desirable to present the possibility of the application of image processing tools to compare the severity of defect growth during operations.

2.4. Risk Assessment

The risk index was calculated by multiplying severity grades with the probability of defects. To this end, the relative durability index was calculated based on the risk index as follows in Figure 2:

$$Risk = P_f \times S_f \tag{6}$$

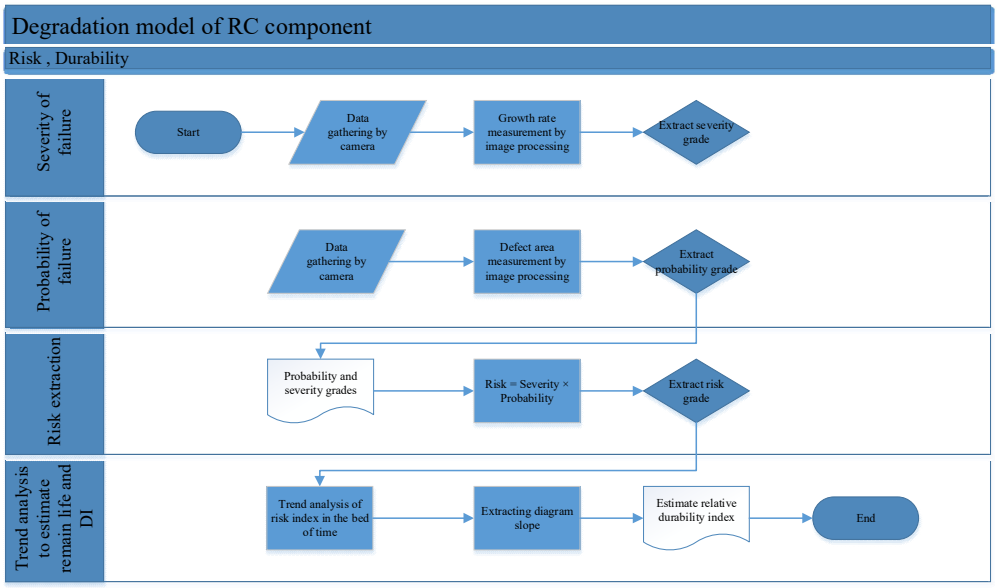

Figure 2. Research method.

3. Research Case Study

Automated visualization evaluates the RC structural elements in terms of its quality in a similar manner to an experienced inspectors' judgment. Furthermore, this method has more measurable tools than the traditional visual inspection in order to extract risk as a relative index to compare bridges and their RC elements. This comparable index based on quantitative outputs extracts the durability index by using image processing tools. Hence, this approach can be used as a practical replacement for experienced observers and inspectors, especially in the subway, which has frequent loads and only short times for maintenance activities. Additionally, it is possible to randomly double-check qualitative traditional inspections. In this manner, seven RC bridges were selected from the Tehran subway and a critical component was defined by pre-posterior analysis. In the end, the analysis focused on the high-risk case for extracting the durability index based on the proposed method.

3.1. Experimental Tests

The first step of this study is gathering data from the object. Other steps of the research process are shown in Figure 3. Additionally, this process will be repeated to find other aspects of structure status based on linking status points over time and estimating the degradation model with the local slope.

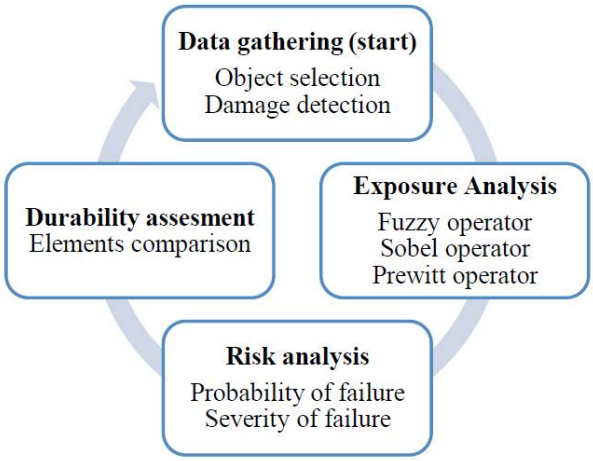

Figure 3. Research process.

3.1.1. Data Gathering

Data gathering with the fixed camera in terms of height and location on the ground was carried out twice. The setup and subject of the case study are illustrated in Figure 4.

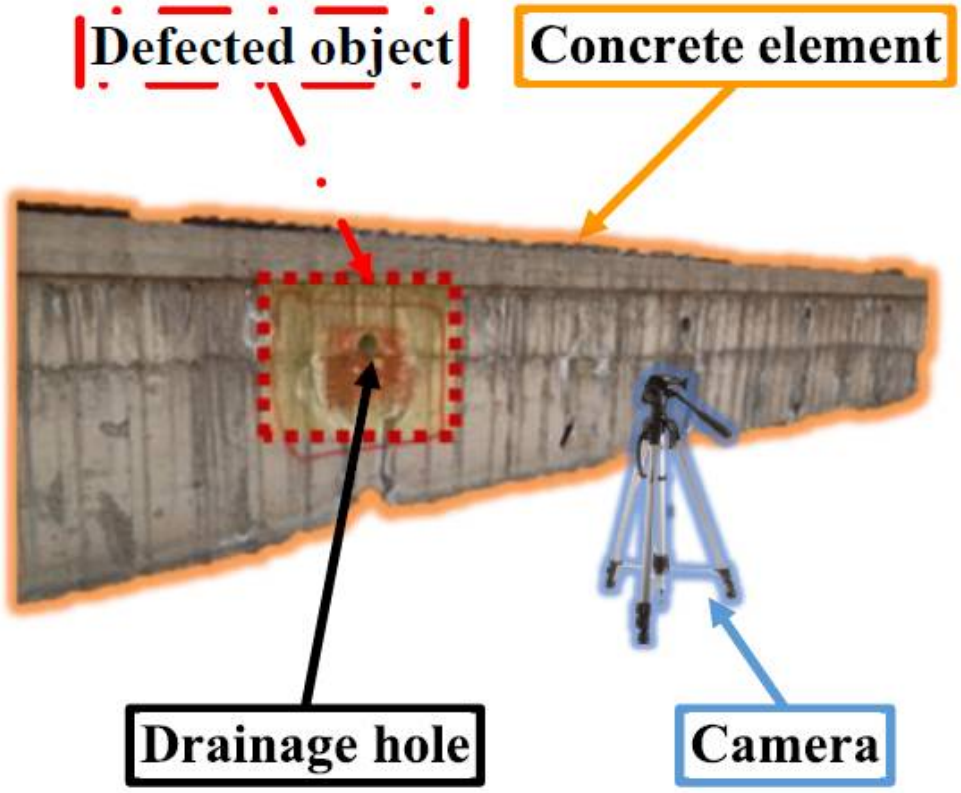

Figure 4. Case study subject–RC element.

When fixing the camera to the ground, the location of its stand was marked for the second data gathering session. Additionally, the drainage hole was a potential place for defect expansion and the extraction of data for the durability index due to these changes was carried out. After a comparison of the images, significant changes were found to exist between the first data gathering session and the second, which was encouraging for the research aim.

The RC elements might be damaged on the surface due to environmental reasons, poor construction quality, bad curing, and other internal or chemical damage reasons. The surface damage is as follows:

- Cracking;
- Crazing;
- Blistering;
- Delamination;
- Dusting;
- Curling;
- Efflorescence;
- Scaling and spalling.

It is necessary to mention these surface damages are considered a threat to concrete durability.

3.1.2. Exposure Analysis

After data gathering and pre-posterior analysis, it is necessary to analyze surface damage to assess exposed defects [44]. The critical zone was selected based on initial data gathering and the abutment of the bridge. The durability feature has a direct link with the surface defect and drainage location is a potential point for surface damage. The traditional

method relies on subjective interpretation based on visual inspection. Meanwhile, image processing software monitors the rate of defect expansion. Figure 5A,B illustrates the result of this analysis.

The measurement of the damaged area has been carried out using automated software in this research. Although the surface of the concrete is intact at the first step of data gathering, this zone is exposed to wastewater due to poor drainage design and damage over time.

Therefore, the first row in Figure 5A,B (number 1–4) depicts intact concrete before surface damage at the first step of gathering data. The second row in both pictures (number 5–8) demonstrates the damaged surface over time. Therefore, based on Figure 5A, the damages reveal minor damage over a short time. Figure 5B shows significant defects over a longer time when compared to the first image. The third row (number 9–12) is a result of a comparison between intact concrete and damaged concrete over time. As the first data gathering session, based on Figure 5A, revealed a minor defect in a short time, the damaged area is smaller than in the second data gathering session seen in Figure 5B after a longer time. Additionally, the first column in Figure 5A,B (number 1, 5 and 9) demonstrates the greyscale and pure image of the object without noise. The second column (number 2, 6 and 10) shows the result of image processing through fuzzy logic. The third column (4, 8 and 12) illustrates the image processing analysis and comparison using the Sobel algorithm, and finally, the fourth column (number 4, 8 and 12) is the output of the comparison by the Prewitt operator. The software output comprises a comparison between damaged and intact surfaces and is verified by double-checking using manual measurement tools.

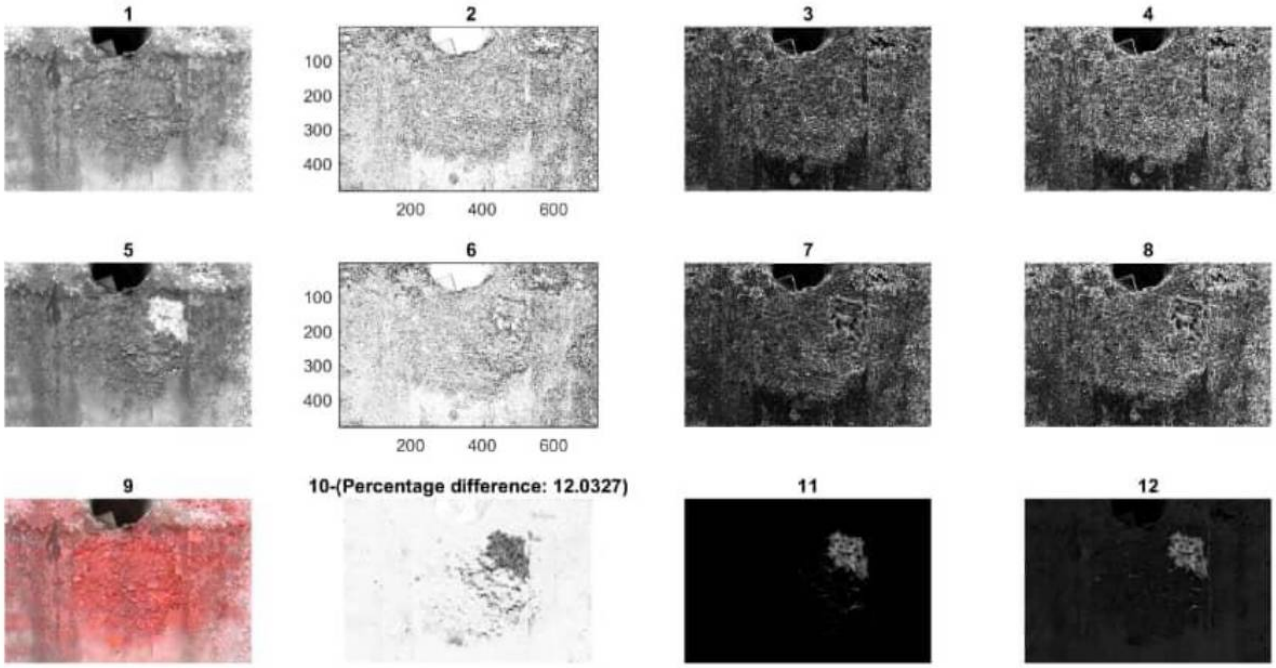

(**A**)

Figure 5. *Cont.*

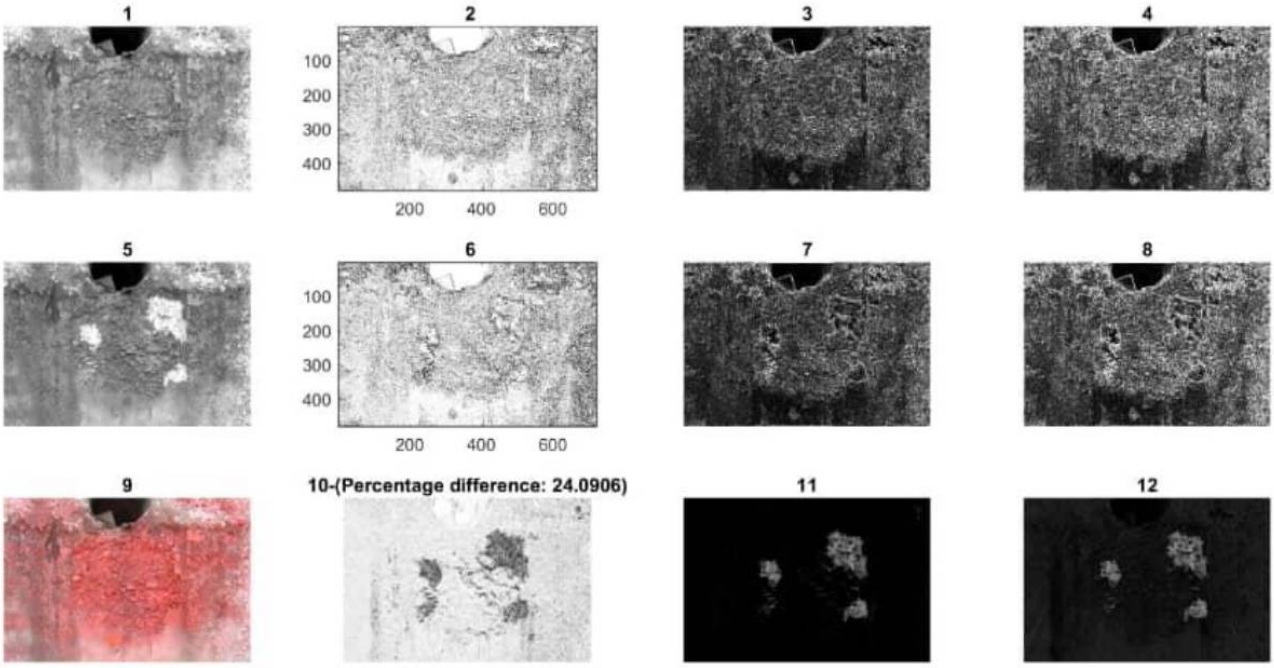

(**B**)

Figure 5. (**A**) Surface concrete with a minor defect. (**B**) Surface concrete with a major defect.

3.1.3. Discussion

In this research, seven RC bridges from the Tehran subway railway network were selected and checked. The riskiest bridge has been selected for detailed inspection and monitoring over time.

I. Probability of Failure (P_f)

To extract the probability of failure, it is possible to count the number of defects in each component divided by their approximate volume, and the probability of failure (P_f) is updatable in each time window. To find a critical case, seven RC bridges were checked during pre-posterior analysis. The probability of failure in each bridge was calculated based on their approximate volume according to Table 1.

Table 1. Approximate volume of elements for risk assessment.

Bridge	Pier Type	Span Number	Average Span Length (m)	Abutment Height (m)	Bridge Width (m)	Bridge Length (m)	Deck Area (m^2)	Material Volume (m^3)
1	-	1	15.6	4	12	15.6	187.2	748.8
2	Wall, Single pier	1	15.6	5	9.14	15.6	142.584	712.92
3	Several in each section, Cylinder	5	15.6	3	9.06	78	706.68	5653.44
4	-	1	15.6	4	9.1	15.6	141.96	709.8
5	Several in each section, Cylinder	1	19.8	7	12	79.2	950.4	6652.8
6	Several in each section	1	15.6	12	9.13	15.6	142.428	854.568
7	-	1	12.6	6	9.06	12.6	114.156	684.936

Based on the approximate volume and the quantity of the damaged area on the material in question, the probability of failure in each element was estimated during the visual inspection, as is shown in Tables 2 and 3A,B.

Table 2. Superstructure probability of failure for risk assessment.

Bridge	Number of Damaged Area on Deck			Failure Density of Deck	Probability of Failure (Deck) 0–1
	Barriers	Beams	Drainage		
1	0	0	0	0	0
2	0	1	0	0.007013	0.118714
3	0	2	2	0.00566	0.095809
4	0	2	1	0.021133	0.357706
5	1	2	1	0.004209	0.07124
6	0	2	1	0.021063	0.356531
7	0	0	0	0	0

Table 3. (**A**) Probability of failure for substructure, part 1. (**B**) Probability of failure for substructure, part 2.

(A)			
Bridge	Elements of Abutment		
	Number of Damaged Areas	Failure Density of Abutment	Probability of Failure (Abutment) 0–1
1	0	0	0
2	0	0	0
3	1	0.25	0.5
4	0	0	0
5	1	0.25	0.5
6	0	0	0
7	0	0	0

(B)					
Bridge	Foundation			Elements of Pier	
	Number of Damaged Areas Pedestal	Footing	Probability of Failure (Foundation) 0–1	Number of Damaged Areas Elastomeric Bearing	Probability of Failure (Pier) 0–1
1–7	0	0	0	0	0

II. Severity of Failure (S_f)

Therefore, after finding the critical component of the bridges based on P_f, it is possible to find S_f according to the results of the automated visual inspection, and then it is possible to calculate the risk and durability index.

The results based on Figure 5 were analyzed according to the estimated damage growth and critical zone severity for risk. The rate of damage growth in critical elements based on damage expansion are presented in Table 4.

Table 4. Damage growth in the abutment of the critical bridge element.

No.	Year	Month (T)	Damage Growth (S_f)	P_f	Risk (R_t)
1	0	0	0	0.5	-
2	0.25	3	0.12		0.6
3	0.5	6	0.24		0.12
4	1	12	0.48 (Estimation)		0.24

These results present the severity of failure in the critical element of the bridge with the highest P_f.

III. Risk Grades and Durability Index

Since durability as a time-dependent probabilistic reliability may be prolonged by the repairs of materials and components, it is necessary to consider temporary durability [45].

Meanwhile, according to Figure 6, RC component degradation intensity status changes over an element's lifespan. This means that the durability index has to change in each period, not only based on repair activities but also according to a component's period of life.

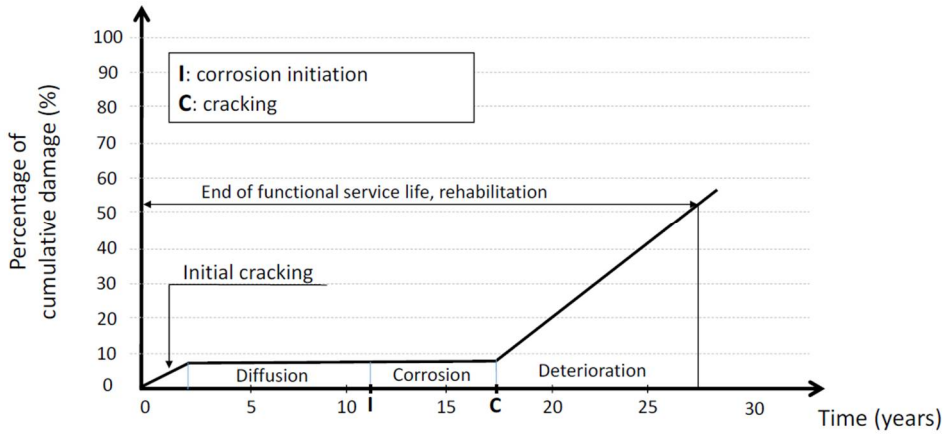

Figure 6. Degradation of reinforced concrete [43].

Therefore, in this research, it is desirable to estimate the tangent line of the function for the degradation model of an RC element in a short period of definite time [46]. To this end, the durability index estimated by the function of risk over time is as follows:

$$D_i = \frac{dR_t}{dt} \tag{7}$$

IV. Results of Case Study Analysis

The degradation model of the RC component is dependent on the durability index and the durability index has a relation to risk over time. Based on recent data extracted from the case study within a short time period, the function of the tangent line is as follows:

$$Y - R_2 = \left(\frac{R_2 - R_1}{T_2 - T_1}\right) X - T_2 \tag{8}$$

In this formula, damage will expand through life. If "Y" is the RC component status in terms of degradation and "X" is a variable based on time, the degradation model estimates are based on temporary durability. Therefore, the risk in operations will change over time, and "T" represents time in terms of the month. "R" denotes the risk based on damage growth within the RC element during operation and the slope of the duration, which represents the D_i in each segment.

4. Conclusions

This research proposed an approach to estimate the output of the degradation model based on the durability index according to the potential risk concerning input data (S_f and P_f). The degradation model is useful for assigning corrective actions for dangerous RC components during emergency conditions. It is also necessary the planning frequent inspections and preventive maintenance in terms of RCM for the quality control of infrastructures.

After pre-posterior analysis and defining risky RC components, the degradation model was estimated based on the durability index. Based on the image processing results, the damage growth rate was 24% during the definite time in this load-bearing RC component. If this definite time spans 6 months, this case had three milestones during the testing. The first data gathering was carried out on the intact RC component, and the second milestone occurred simultaneously with the initial damage growth of 12%. Meanwhile, the final and third milestone with 24% damage was measured by this proposed method. If severity and probability considering for risk calculation, the component durability index will be extracted

based on variable reliability over the life of the component as a degradation model during operation. In other words, if service limit and ultimate limit are considered as thresholds in the degradation model, it is possible to estimate the next step of a structure's status based on the degradation model and compare the next step of the structure status with the expected structure status [25]. In this case, the D_i was estimated at 0.02 for the definite time of inspection as a temporary durability index to estimate the degradation model.

Image processing was exploited as a tool to reach the research aim. Meanwhile, this research not only compares the operators of image processing but also combines the data gathering with mathematical tools and a statistical approach in terms of the risk concept. Merging the data processing in terms of vulnerable zones with image processing tools to find the maximum difference between the image processing operators in each element helps the user to decide on maintenance planning using the hybrid approach. Additionally, this comparison approach maximizes the value of information after data gathering by the image processing operator.

Finding the damage growth and estimating the degradation trend is not possible through traditional visual inspection. More than simply proposing structural health monitoring tools for data gathering, this quantitative method estimates the status of reinforced concrete without in-person observation. Therefore, regardless of human error elimination, the computer records data and trends those data with a risk logic concept to prioritize vulnerable zones based on their degradation rate.

Author Contributions: Study conception and design; data collection; analysis and interpretation of results; draft manuscript preparation: S.M.S.L. Supervising the research project: F.M.N. Research consultant: M.R. All authors have read and agreed to the published version of the manuscript.

Funding: The authors received no financial support for the research, and publication of this article.

Data Availability Statement: All data that support the findings of this study are available from the corresponding author upon reasonable request. Additionally, all data used during the study appear in the submitted article.

Acknowledgments: I would like to express my very great appreciation to Majid Mirbod for his valuable suggestions during the development of this research work. His willingness to give his time so generously has been very much appreciated. Finally, I wish to thank my parents and my wife for their support and encouragement throughout my study.

Conflicts of Interest: The authors declare that they have no known competing financial interests or personal relationships that could have appeared to influence the work reported in this paper.

References

1. Agnisarman, S.; Lopes, S.; Chalil, K.; Piratla, K. Automation in Construction A survey of automation-enabled human-in-the-loop systems for infrastructure visual inspection. *Autom. Constr.* **2019**, *97*, 52–762. [CrossRef]
2. Hui, L.I.; Jinping, O.U. Structural Health Monitoring: From Sensing Technology Stepping to Health Diagnosis. *Procedia Eng.* **2011**, *14*, 753–760. [CrossRef]
3. Fan, G.; Li, J.; Hao, H. Vibration signal denoising for structural health monitoring by residual convolutional neural networks. *Measurement* **2020**, *157*, 107651. [CrossRef]
4. Taheri, S. A review on five key sensors for monitoring of concrete structures. *Constr. Build. Mater.* **2019**, *204*, 492–509. [CrossRef]
5. Yun, H.; Choi, W.; Seo, S. NDT E International Acoustic emission activities and damage evaluation of reinforced concrete beams strengthened with CFRP sheets. *NDT E Int.* **2010**, *43*, 615–628. [CrossRef]
6. Behnia, A.; Kian, H.; Mousa, A.A.; Alireza, S. A novel damage index for online monitoring of RC slabs under monotonic loading by integration of process controlling into acoustic emission technique. *Mech. Syst. Signal Processing* **2019**, *119*, 547–560. [CrossRef]
7. Bagherifaez, M.; Behnia, A.; Majeed, A.A.; Kian, C.H. Acoustic Emission Monitoring of Multicell Reinforced Concrete Box Girders. *Sci. World J.* **2014**, *2014*, 567619. [CrossRef]
8. Tsangouri, E.; Remy, O.; Boulpaep, F.; Verbruggen, S.; Livitsanos, G.; Aggelis, D.G. Structural health assessment of prefabricated concrete elements using Acoustic Emission: Towards an optimized damage sensing tool. *Constr. Build. Mater.* **2019**, *206*, 261–269. [CrossRef]
9. Li, D.; Cong, A.; Guo, S. Automation in Construction Sewer damage detection from imbalanced CCTV inspection data using deep convolutional neural networks with hierarchical classi fi cation. *Autom. Constr.* **2019**, *101*, 199–208. [CrossRef]

10. Biswas, R.; Sil, J. An improved canny edge detection algorithm based on type-2 fuzzy sets. *Procedia Technol.* **2012**, *4*, 820–824. [CrossRef]
11. Wang, Y.; Liu, K.; Wang, C.; Zhou, S. Influence of solution concentration and temperature on the repair effect for electrophoretic deposition of rust-cracked reinforced concrete. *J. Build. Eng.* **2022**, *56*, 104772. [CrossRef]
12. Tabiai, I.; Tkachev, G.; Diehl, P.; Ertl, T.; Therriault, D.; Lévesque, M. Hybrid image processing approach for autonomous crack area detection and tracking using local digital image correlation results applied to single- fi ber interfacial debonding. *Eng. Fract. Mech.* **2019**, *216*, 106485. [CrossRef]
13. Zhang, J.; Yang, X.; Li, W.; Zhang, S.; Jia, Y. Automation in Construction Automatic detection of moisture damages in asphalt pavements from GPR data with deep CNN and IRS method. *Autom. Constr.* **2020**, *113*, 103119. [CrossRef]
14. Dinh, K.; Gucunski, N.; Zayed, T. NDT and E International Automated visualization of concrete bridge deck condition from GPR data. *NDT E Int.* **2019**, *102*, 120–128. [CrossRef]
15. Nejati, A.; Ravanshadnia, M.; Sadeh, E. Selecting an Appropriate Express Railway Pavement System Using VIKOR Multi-Criteria Decision Making Model. *Civ. Eng. J.* **2018**, *4*, 1104–1116. [CrossRef]
16. Jadidi, H.; Ravanshadnia, M.; Hosseinalipour, M.; Rahmani, F. A step-by-step construction site photography procedure to enhance the efficiency of as-built data visualization: A case study. *Vis. Eng.* **2015**, *3*, 1148. [CrossRef]
17. Shalabi, F.; Turkan, Y. IFC BIM-Based Facility Management Approach to Optimize Data Collection for Corrective Maintenance. *J. Perform. Constr. Facil.* **2017**, *31*, 04016081. [CrossRef]
18. Chong, H.Y.; Wang, J.; Shou, W.; Wang, X.; Guo, J. Improving Quality and Performance of Facility Management Using Building Information Modelling. In *Cooperative Design, Visualization, and Engineering*; CDVE 2014. Lecture Notes in Computer Science; Luo, Y., Ed.; Springer: Cham, Switzerland, 2014; Volume 8683. [CrossRef]
19. Boukamp, F.; Akinci, B. Automated processing of construction specifications to support inspection and quality control. *Autom. Constr.* **2007**, *17*, 90–106. [CrossRef]
20. Kim, M.K.; Wang, Q.; Park, J.W.; Cheng, J.C.P.; Sohn, H.; Chang, C.C. Automated dimensional quality assurance of full-scale precast concrete elements using laser scanning and BIM. *Autom. Constr.* **2016**, *72*, 102–114. [CrossRef]
21. Singh, V.; Gu, N.; Wang, X. A theoretical framework of a BIM-based multi-disciplinary collaboration platform. *Autom. Constr.* **2011**, *20*, 134–144. [CrossRef]
22. Mohammad, S.; Lajevardi Lourenço, P.B.; Sousa, H.S.; Matos, J.C. Railway Reinforced concrete infrastructure life management and sustainability index. *Acta Polytech. CTU Proc.* **2022**, *33*, 316–321. [CrossRef]
23. Stehlík, M. Enhancing the durability of concrete made of concrete recyclate by additives and admixtures. *J. Civil Eng. Manag.* **2014**, *20*, 270–279. [CrossRef]
24. *AASHTO T 210-91*; Durability Index of Aggregates. American Association of State and Highway Transportation Officials: Washington, DC, USA, 2015.
25. The International Organization for Standardization. *Durability—Service Life Design of Concrete Structures (ISO 16204)*; International Standard: Geneva, Switzerland, 2012.
26. Vořechovská, D.; Teplý, B.; Chromá, M. Probabilistic Assessment of Concrete Structure Durability under Reinforcement Corrosion Attack. *J. Perform. Constr. Facil.* **2010**, *24*, 571–579. [CrossRef]
27. Zou, D.; Wang, Z.; Shen, M.; Liu, T.; Zhou, A. Improvement in freeze-thaw durability of recycled aggregate permeable concrete with silane modification. *Constr. Build. Mater.* **2021**, *268*, 121097. [CrossRef]
28. Azarsa, P.; Gupta, R. Resistivity of Concrete for Electrical Durability Evaluation: A Review. *Adv. Mater. Sci. Eng.* **2017**, *2017*, 8453095. [CrossRef]
29. Carino, N.J. Nondestructive Techniques to Investigate Corrosion Status in Concrete Structures. *J. Perform. Constr. Facil.* **1999**, *13*, 96–106. [CrossRef]
30. Lajevardi, S.; Matos, J.; Lourenço, P.B. Quality control index survey for railway bridge health monitoring. In Proceedings of the IABSE Symposium Towards a Resilient Built Environment Risk and Asset Management, Guimaraes, Portugal, 27–29 March 2019; pp. 317–326.
31. Jokūbaitis, A.; Valivonis, J.; Marčiukaitis, G. Analysis of Strain State and Cracking of Cocnrete Sleepers. *J. Civil Eng. Manag.* **2016**, *22*, 564–572. [CrossRef]
32. Sadegh, L.; Sousa, H.; Lourenco, P.; Matos, J.; Oliveira, D. Operation reliability index for maintenance decision making in bridges. In Proceedings of the International Istanbul Bridge Conference, Online, 16–17 November 2020.
33. Canny, J. A Computational Approach to Edge Detection. *IEEE Trans. Pattern Anal. Mach. Intell.* **1986**, *PAMI-8*, 679–698. [CrossRef]
34. Almeida, G.; Melício, F.; Biscaia, H.; Chastre, C.; Fonseca, J.M. In-Plane Displacement and Strain Image Analysis. *Comput.-Aided Civ. Infrastruct. Eng.* **2016**, *31*, 292–304. [CrossRef]
35. Zhang, D.; Xu, X.; Lin, H.; Gui, R.; Cao, M.; He, L. Automation in Construction Automatic road-marking detection and measurement from laser-scanning 3D profile data. *Autom. Constr.* **2019**, *108*, 102957. [CrossRef]
36. Mahler, D.S.; Kharoufa, Z.B.; Wong, E.K.; Shaw, L.G. Pavement Distress Analysis Using Image Processing Techniques. *Comput.-Aided Civ. Infrastruct. Eng.* **1991**, *6*, 1–14. [CrossRef]
37. Spencer, B.F.; Hoskere, V.; Narazaki, Y. Advances in Computer Vision-Based Civil Infrastructure Inspection and Monitoring. *Engineering* **2019**, *5*, 199–222. [CrossRef]

38. Khunteta, A.; Ghosh, D. Edge Detection via Edge-Strength Estimation Using Fuzzy Reasoning and Optimal Threshold Selection Using Particle Swarm Optimization. *Adv. Fuzzy Syst.* **2014**, *2014*, 365817. [CrossRef]
39. Amza, C.G.; Cicic, D.T. Industrial image processing using fuzzy-logic. *Procedia Eng.* **2015**, *100*, 492–498. [CrossRef]
40. Fageth, R.; Allen, W.G.; Jäger, U. Fuzzy logic classification in image processing. *Fuzzy Sets Syst.* **1996**, *82*, 265–278. [CrossRef]
41. Chen, Z.P.; Guang, C.; Wang, Y.; Zhang, J.Y. Research crack detection of algorithm of the concrete bridge based on image processing. *Procedia Comput. Sci.* **2019**, *154*, 610–616. [CrossRef]
42. Gonzalez, R.; Woods, R. *Digital Image Processing*; Addison Wesley: Boston, MA, USA, 1992; pp. 414–428.
43. Lakhani, K.; Minocha, B.; Gugnani, N. Analyzing edge detection techniques for feature extraction in dental radiographs. *Perspect. Sci.* **2016**, *8*, 395–398. [CrossRef]
44. Ebadi, M.; Bagheri, M.; Lajevardi, M.S.; Haas, B. Defect Detection of Railway Turnout Using 3D Scanning. In *Sustainable Rail Transport*; Fraszczyk, A., Marinov, M., Eds.; Lecture Notes in Mobility; Springer: Cham, Switzerland, 2019. [CrossRef]
45. Kliukas, R.; Kudzys, A. Probabilistic durability prediction of existing building elements. *J. Civil Eng. Manag.* **2004**, *10*, 107–112. [CrossRef]
46. Liu, Y.; Weyers, R.E. Modeling time-to-corrosion cracking in chloride contaminated reinforced concrete structures. *ACI Mater. J.* **1999**, *96*, 611–613.